arXiv:1610.03318v1 [cond-mat.mtrl-sci] 11 Oct 2016

Determination of hole g-factor in InAs/InGaAs/InAlAs quantum wells by magneto-photoluminescence studies

Ya. V. Terent'ev[1,2], S. N. Danilov[1], M. V. Durnev[2], J. Loher[1], D. Schuh[1], D. Bougeard[1], S. V. Ivanov[2], and S. D. Ganichev[1]
[1] *Physics Department, University of Regensburg, 93040 Regensburg, Germany and*
[2] *Ioffe Institute, 194021 St. Petersburg, Russia*

Circularly-polarized magneto-photoluminescence (magneto-PL) technique has been applied to investigate Zeeman effect in InAs/InGaAs/InAlAs quantum wells (QWs) in Faraday geometry. Structures with different thickness of the QW barriers have been studied in magnetic field parallel and tilted with respect to the sample normal. Effective electron-hole g-factor has been found by measurement of splitting of polarized magneto-PL lines. Landé factors of electrons have been calculated using the 14-band $\boldsymbol{k}\cdot\boldsymbol{p}$ method and g-factor of holes was determined by subtracting the calculated contribution of the electrons from the effective electron-hole g-factor. Anisotropy of the hole g-factor has been studied applying tilted magnetic field.

I. INTRODUCTION

Heterostructures based on InAs possess series of unique properties caused by a narrow bandgap. These properties include high carrier mobility and a strong spin-orbit interaction making the system a promising candidate for high frequency electronics, optoelectronics and spintronics application. One of the most interesting objects in this area are type-I quantum wells (QWs) based on a InAs/InGaAs/InAlAs two-step bandgap engineering, where In content can be varied from 30 to 80% [1]. Such structures exhibit bright photoluminiscence in mid-infrared range [2, 3] demonstrate high-mobility two-dimensional electron gas [4–7], pronounced spin-dependent optical [3, 8, 9] and transport [10–15] phenomena. Determination of Landé factors of both types of the carriers is the cornerstone for the studies of spin-related phenomena. As for InAs QWs, electron g-factor in this type of heterostructures is well-studied by different techniques. To date, reported values of electron g-factor obtained by magneto-transport and terahertz experiments range from g_e= -3 to g_e= -9 depending on In content in QW barrier [6, 11, 12]. Moreover, experimentally obtained Landé factors are consistent with the values calculated in the framework of $\boldsymbol{k}\cdot\boldsymbol{p}$ method.

In contrast to electrons, determination of the hole g-factor g_h is still a challenging task. There are no available experimental data as well as reliable theoretical calculations. The picture becomes even more intriguing in light of the previous magneto-optical experiments [3, 8]. They indicate surprisingly small magnitude of the effective electron-hole g-factor which is the difference between g_h and g_e.

Here we report on studies of $InAs/In_{0.75}Ga_{0.25}As/In_{0.75}Al_{0.25}As$ QW structures by polarization-resolved magneto-PL, which enables direct measurement of effective electron-hole g-factor. We have determined Landé factor of holes combining obtained experimental data with theoretical calculations of an electron contribution. We have obtained the dependence of electron and hole g-factors on QW barrier width. We have investigated anisotropy of the hole g-factor in tilted magnetic field, and shown that the values of g_h in tilted magnetic field are in agreement with prediction of close-to-zero hole Zeeman splitting in magnetic field lying in QW plane.

II. SAMPLES AND EXPERIMENTAL TECHNIQUE

Experimental samples were fabricated by molecular beam epitaxy onto a fully relaxed $In_xAl_{1-x}As$/(001)GaAs graded buffer [3, 16] with a stepwise increase of the In content (x = 0.05 to x = 0.75) over 1 μm. The structure of QW is sketched in the inset of Fig. 1. An $In_{0.75}Ga_{0.25}As$ quantum size part embedded in between $In_{0.75}Al_{0.25}As$ layers features a symmetrically inserted and compressively strained InAs QW of 4 nm. A set of samples with the different thickness of $In_{0.75}Ga_{0.25}As$ barrier a was grown, where a is set to 7, 2.5 and 0 nm. The corresponding structures are labeled A, B and C.

PL was excited by emission of a laser diode operating in the *cw* mode at wavelength $\lambda = 809$ nm and detected with a Fourier Transform Infrared (FTIR) spectrometer. The laser beam was focused to a 1-mm diameter spot on the sample. The excitation intensity W_{exc} was 100 mW. An external magnetic field up to 6 T was applied perpendicularly to the wafer or was inclined at an angle of 40° to the direction of sample growth. PL emission having wave vector directed along magnetic field was detected (Faraday geometry). The sample temperature was kept as low as 2 K. Right- and left-handed circular polarized emission spectra were recorded applying a quarter wave ZnSe Fresnel rhomb [17, 18].

III. EXPERIMENTAL RESULTS

Bright PL was detected from all the samples. Its contour is close to Gaussian function and slightly asymmet-

ric being broadened at low energy slope, see Fig. 1. PL peak energy takes the value of 582.6 meV, 616.5 meV and 713.6 meV in structures A, B and C, respectively. So PL peak energy increases with decrease of InGaAs barrier width. Emission intensity also varies in samples with different barrier width and decays with its reduction. Both trends correlate with increase of PL peak full width at half maximum (FWHM) that takes the value of 18, 22 and 40 meV, in samples A, B and C, respectively. Application of external magnetic field $\boldsymbol{B}$ in direction perpendicular to QW plane results in substantial changes in the PL spectrum. It experiences magnetic-field-induced splitting into circular polarized components, which is different in structures A, B and C, see Fig. 2. Similar to PL peak energy and FWHM, the splitting depends on InGaAs barrier width. It is extremely small in structure A with the largest InGaAs barrier but is well-pronounced in sample C, where this layer is absent, taking intermediate value in structure B. Interestingly, the splitting is a non-linear function of the magnetic field and its dependence on magnetic field is different in all three samples, see Fig. 2. Note that minimal circular polarization of PL

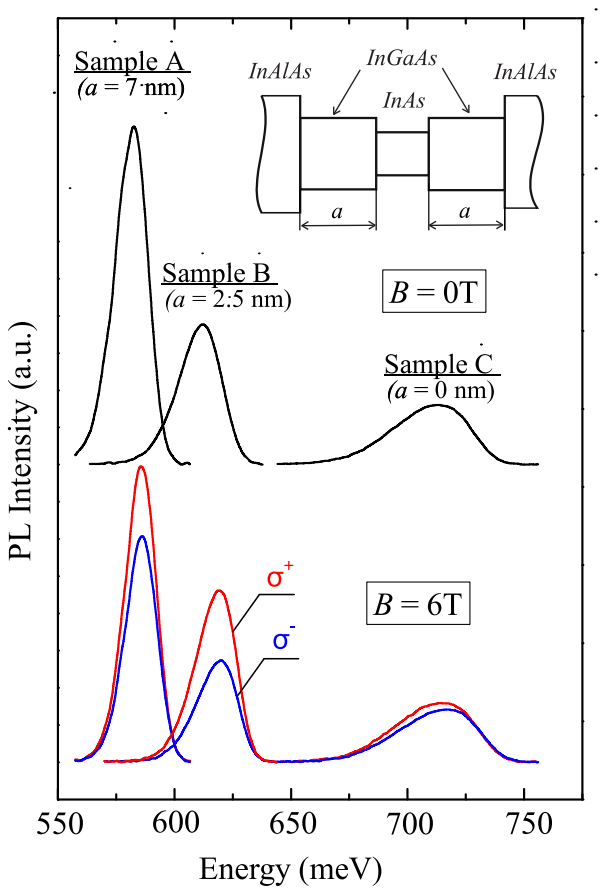

FIG. 1: Photoluminescence spectra and circular-polarized magneto-PL spectra of samples A, B and C with different width of InGaAs barriers, measured at magnetic field $B = 6$ T perpendicular to QW plane. The inset shows the band diagram of the samples active region.

emission was detected in structure C while it possesses the largest splitting. The inclination of the magnetic field used for the analisis of g_h anisotropy critically diminishes the splitting of a magneto-PL peak in samples B and C, however does not affect it in sample A, see Fig. 2.

Besides the splitting of the PL contour into circular-polarized components, emission spectra experience blue shift, which corresponds to the diamagnetic shift of electron and hole energy levels in magnetic field. The shift has a quadratic dependence on the magnetic field, see Fig. 3.

IV. DISCUSSION

The observed PL peak originates from direct optical transitions between the ground electron $e1$ and the heavy hole $hh1$ subbands, according to calculations of the optical transition energy. It is important to note, that in our case optical transitions between free-carrier states dominate, in contrast to wide band systems, where the exciton recombination prevails [3].

Observed in experiment quadratic magnetic field dependence of the PL peak diamagnetic shift (Fig. 3) indicates Coulomb localization of the photoexcited carriers [19, 20]. In our structures carriers can be trapped to localization centers which emerge due to inhomogeneity of the InAs QW or presence of charged centers at the interfaces of QW.

Detected splitting of PL lines in two circular polarizations reflects spin splitting of conduction and valence bands. The linear region of the Zeeman splitting (see Fig. 2) gives the value of the effective electron-hole g-factor (g_{eff}), which is equal to the difference of g-factors of the carriers that take part in the optical recombination, $g_{\text{eff}} = g_h - g_e$ [3]. The extracted values of g_{eff} as a function of an InGaAs barrier width are presented in Fig. 4 and Tab. I. It is clearly seen that the absolute value of g_{eff} tends to increase with decreasing width of InGaAs barrier.

While observed nonlinear character of Zeeman splitting in magnetic field $B \gtrsim 2$ is out of scope of present paper, it is worth mentioning that highly nonlinear Zeeman splitting of excitons was also detected in AlGaAs/GaAs and InGaAs/GaAs systems and the model was suggested that is based on a spin-dependent field-induced admixture between the light- and heavy-hole valence bands [22].

Large FWHM of the PL peak and its decay detected in sample C is explained in terms of effective scattering by charged centers at QW interfaces. In this structure QW interfaces are formed by InAs and InAlAs layers having large lattice mismatch and therefore are characterized by large defects density. Apparently scattering on these defects is responsible for the strong decay of optical recombination efficiency, increase of FWHM as well as depolarization of the emission in the case of the magnetic field applied.

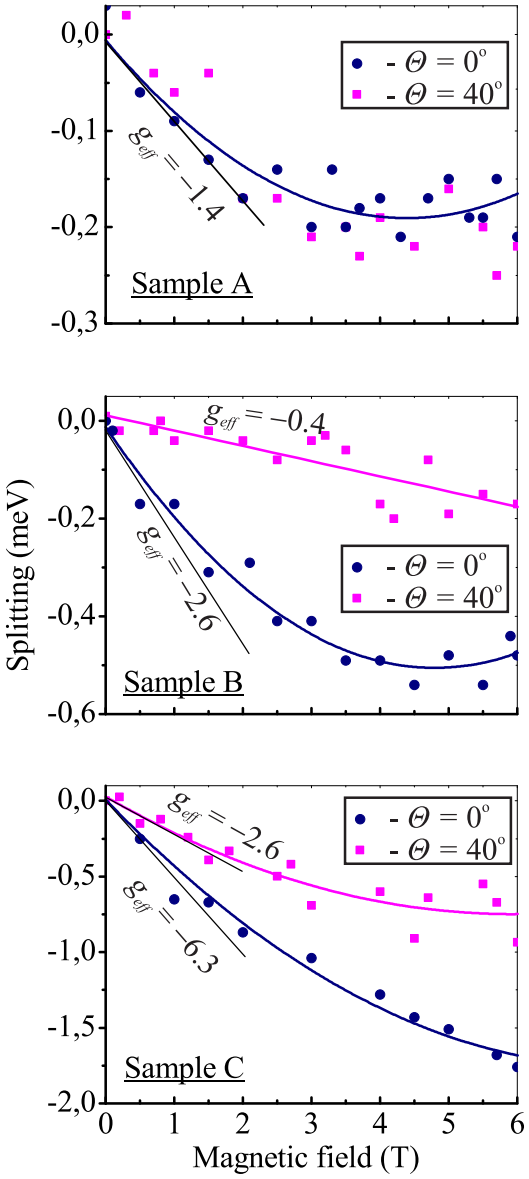

FIG. 2: Zeeman splitting of magneto-PL peak for structures A, B and C with different width of InGaAs barriers measured at magnetic field perpendicular to QW plane and tilted by $\theta = 40^\circ$ with respect to the sample normal. Curves present polynomial fit to the experimental points. Straight lines show linear fit at small magnetic fields, which gives effective g-factors of free carriers.

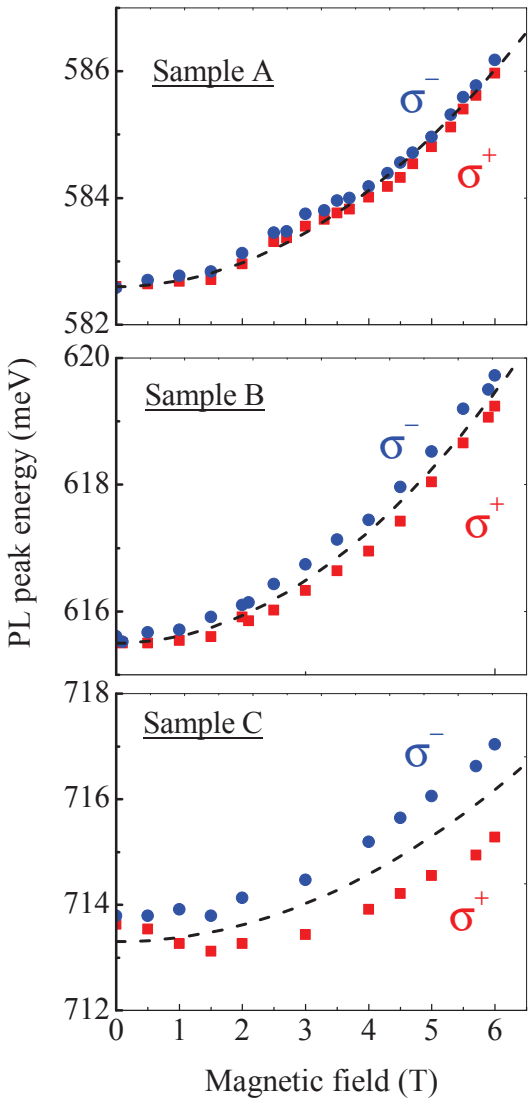

FIG. 3: Circular polarized PL peaks energies as a function of magnetic field. Curves present parabolic fitting $E = \alpha_{\rm dia} B^2$ of the diamagnetic shift of PL lines, which is determined as a half-sum of the σ^+ and σ^- components. The values of $\alpha_{\rm dia}$ are listed in Tab. I.

Now we turn to separate determination of electron and hole g-factors. It was found that the g-factor of hole is extremely sensitive to the separation between heavy-hole and light-hole quantization levels, which in turn depends on the unknown strength of strain fields and localization potential. Hence we only calculate g_e, which is less affected by the localization potential and strain, and therefore can be evaluated with much higher accuracy. Then we estimate the value of g_h using experimentally determined $g_{\rm eff}$ and

$$g_{\rm eff} = g_h - g_e \,. \qquad (1)$$

Computation method is based on numeric diagonalization of the 14-band $\boldsymbol{k}\cdot\boldsymbol{p}$ Hamiltonian in the presence of magnetic field [23, 24]. We use the developed in Ref. [23] 14-band $\boldsymbol{k}\cdot\boldsymbol{p}$-model for calculation of electron and hole states at zero magnetic field, and use obtained wave functions to calculate the Zeeman splitting at small magnetic fields in the framework of perturbation theory (the approach is analogous to the one used to calculate heavy-hole and light-hole g-factors in the framework of Luttinger Hamiltonian, see Eqs. (9a), (9b) of Ref. [24]). The band parameters of InAs and its alloys were taken from Refs. [25, 26], and confining potentials for electron and

TABLE I: The values of electron and hole g-factors ($g_{\rm eff}$, g_e, g_h) and diamagnetic shifts ($\alpha_{\rm dia}$) extracted from the analysis of experiment. The values g_e^* and g_h^* are derived using Eq. (3) from the analysis of Zeeman splitting in tilted magnetic field.

	Sample A	Sample B	Sample C
$g_{\rm eff}$	-1.4	-2.6	-6.3
g_e	-11	-10.7	-8.4
g_h	-12.4	-13.3	-14.7
g_e^*	–	-9	-13.2
g_h^*	–	-9.4	-15.8
$\alpha_{\rm dia}$ (meV/T^2)	0.095	0.11	0.08

holes were calculated using the model of Ref. [26] taking into account elastic strain present in the structure. The interband matrix elements of momentum operator were taken from Ref. [27].

The evaluated band diagram, wave function of heavy hole at zero in-plane momentum $\boldsymbol{k}_\parallel = 0$, and optical transitions energies are presented in Fig. 5. Theoretical model gives close-to-experiment values of optical transitions energies and the in-plane electron mass m_e ($m_e = 0.038\, m_0$ as determined from transport measurements in similar structures [4, 6, 10]). It also provides a good agreement between theoretical and experimentally measured values of g_e [6, 10, 28]. The discrepancy between theoretically calculated and experimental values of optical transitions energies is possibly attributed to the presence of in-plane localization potentials, which lead to increase of the PL peak energy.

Evaluated values of hole Landé factors g_h as well as theoretical values of g_e and experimentally measured $g_{\rm eff}$ are presented in Fig. 4 and Tab. I. As we mentioned above theoretical calculations do not allow to obtain g_h with sufficient precision. Its values obtained in the framework of 14-band $\boldsymbol{k}\cdot\boldsymbol{p}$-model, used for evaluation of g_e, lie in the range of $g_h = -2 \div -8$ for the studied structures [28], and differ significantly from those given in Tab. I.

In order to study anisotropy of hole g-factor we have carried out experiments in a tilted magnetic field. While electron Zeeman splitting is known to be almost independent of the direction of applied magnetic field [31], the spin splitting of a heavy hole bound to QW potential must be sensitive to a normal component of magnetic field only, because the in-plane heavy-hole g-factor is close to zero in III-V quantum wells [32]. Hence tilted magnetic field should result in modification of $g_{\rm eff}$. Indeed, heavy-hole g-factor in a magnetic field tilted by an angle θ with respect to QW normal is

$$\tilde{g}_h(\theta) = \sqrt{g_h^2 \cos^2\theta + g_{h,\parallel}^2 \sin^2\theta}\,, \qquad (2)$$

where g_h and $g_{h,\parallel}$ are the components of the g-factor tensor for $\boldsymbol{B}$ parallel to the growth axis $z \parallel [001]$ and $\boldsymbol{B}$ oriented in the plane of QW. Since $g_{h,\parallel}$ is close to zero, $\tilde{g}_h \approx g_h \cos\theta$ and its absolute value must be reduced at $\theta \neq 0$.

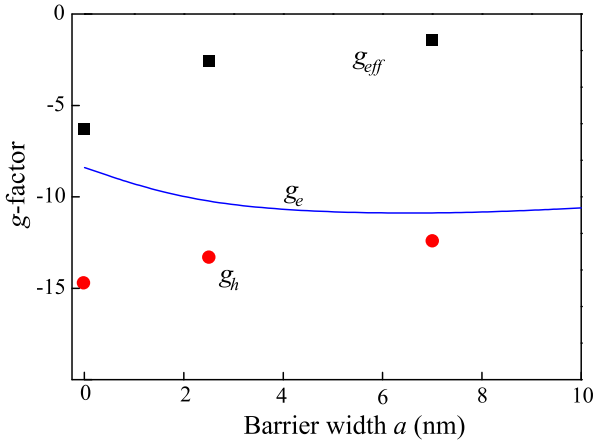

FIG. 4: g-factors in samples under study: squares represent the experimentally measured effective electron-hole g-factor $g_{\rm eff}$, the solid line stands for the theoretically calculated electron g-factor, and circles show the heavy-hole g-factor derived using formula $g_h = g_{\rm eff} + g_e$.

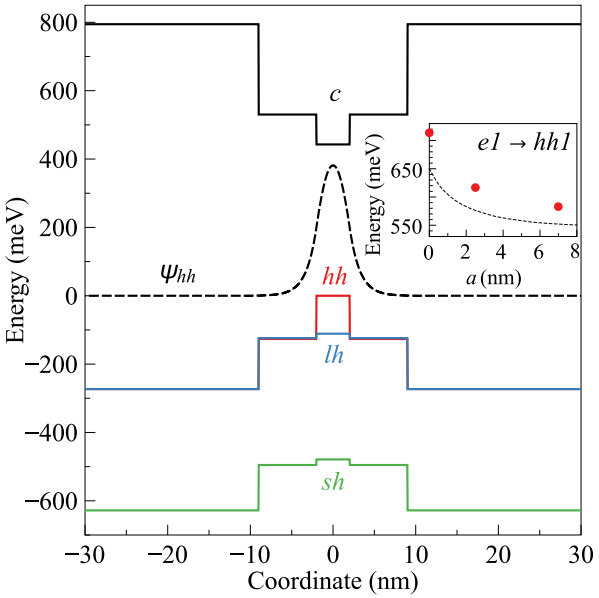

FIG. 5: Band diagram of the quantum well with $a = 7$ nm. The heavy-hole wave function is shown by dashed line. The inset demonstrates the calculated optical transition energy (dashed line) and the experimental points for three samples under study.

For example, the 40° tilt of the field is expected to result in reduction of g_h from -13.3 and -14.7 to -10.2 and -11.3 for samples B and C, respectively. In turn, assuming g_e is independent of θ, the value of $g_{\rm eff}$ is predicted to change to 0.5 and -2.9 for these samples. Comparison with Fig. 2 shows that these estimated values are close to the values observed in experiment.

Anomalous behaviour of the Zeeman splitting was observed in structure A only. As seen from Fig. 2, the effective Zeeman splitting is almost unaffected by the tilt of

$\boldsymbol{B}$ in this sample. It may indicate, that the heavy hole in this sample is localized by rather a three dimensional potential than the potential of QW. This suggestion is consistent with the value of the in-plane localization length of hole $l_h \approx 10$ nm (see below for details), which in the case of sample A is less than the effective localization in the z-direction (see Fig. 5). The possible source for such a three-dimensional confinement is a Coulomb potential of charged centers in quantum well layers.

With the use of Eqs. (1) and (2) it is possible to evaluate g_h and g_e independently without theoretical calculations by measuring $g_{\rm eff}$ at two different angles θ:

$$\begin{aligned} g_h &= \frac{g_{\rm eff}(\theta_1) - g_{\rm eff}(\theta_2)}{\cos\theta_1 - \cos\theta_2}\,, \\ g_e &= \frac{g_{\rm eff}(\theta_1)\cos\theta_2 - g_{\rm eff}(\theta_2)\cos\theta_1}{\cos\theta_1 - \cos\theta_2}\,. \end{aligned} \tag{3}$$

The calculated values are presented in Tab I.

Let us finally analyze the diamagnetic shift of PL lines, see Fig. 3. The value of diamagnetic shift is given by a half-sum of the σ^+ and σ^--polarized components and is well fitted by the quadratic function $E_{\rm dia} = \alpha_{\rm dia} B^2$. The extracted values of $\alpha_{\rm dia}$ are listed in Tab. I. To derive theoretical expression for $\alpha_{\rm dia}$ we will use a simple model of the carriers bound by a parabolic in-plane potential in the form [20, 21]

$$V(\boldsymbol{r}_n) = \frac{\hbar^2}{2m_n l_n^2}\frac{r_n^2}{l_n^2}\,, \tag{4}$$

where $\boldsymbol{r}_n$ is the in-plane coordinate, m_n is the effective in-plane mass, l_n is the in-plane localization length of an electron ($n = e$) and heavy-hole ($n = h$), and $\hbar$ is the Planck constant. Making the Peirels substitution for the carrier wave vector in magnetic field and solving the Schrödinger equation with potential (4) we find for the diamagnetic coefficient $\alpha_{{\rm dia},n}$

$$\alpha_{{\rm dia},n} = \frac{e^2 l_n^2}{8 m_n c^2}\,, \tag{5}$$

where e is the electron charge, and c is the speed of light. Since in QWs under study $m_e \ll m_h$ (electron mass $m_e = 0.038\, m_0$ [4, 6, 10], heavy-hole mass $m_h = 0.085\, m_0$ is deduced from the $\boldsymbol{k}\cdot\boldsymbol{p}$ calculations for sample A) we conclude that the main contribution to the diamagnetic shift results from a confined electron. Taking experimentally measured values of $\alpha_{\rm dia}$ we find that the in-plane localization length for an electron is $l_e \approx 13$ nm in all studied samples. Localization length for a hole is $l_h = (m_e/m_h)^{1/4} l_e \approx 10$ nm and is even smaller than l_e.

V. CONCLUSIONS

To summarize, series of magneto-optical experiments have been carried out on narrow gap InAlAs/InGaAs/InAs QWs with different width of InGaAs barrier in both perpendicular and tilted magnetic fields. Effective electron-hole g-factor is measured directly from the splitting of magneto-PL line into circularly-polarized terms. The values of electron g-factor g_e are calculated theoretically while the g-factor of holes is estimated by extracting g_e from the total splitting. Experiments in tilted magnetic field were used to investigate anisotropy of the heavy hole g-factor.

Acknowledgments

The authors are grateful to S. A. Tarasenko for interest in the work and useful discussions.

The authors gratefully acknowledge financial support from DFG SFB 689, Ya.V.T. and S.V.I. are thankful to the support from RSF (Project 15-12-30022). M.V.D. acknowledges financial support from RFBR project No. 16-32-60175 and the Dynasty foundation.

[1] K. Inoue, J.C. Harmand and T. Matsuno, J. of Cryst. Growth **111**, 313 (1991).
[2] E. Tournié, O. Brandt, and K. Ploog, Appl. Phys. Lett. **60**, 2877 (1992).
[3] Ya. V. Terent'ev, S.N. Danilov, J. Loher, D. Schuh, D. Bougeard, D. Weiss, M.V. Durnev, S.A. Tarasenko, M.S. Mukhin, S.V. Ivanov, and S.D. Ganichev, Appl. Phys. Lett. **104**, 101111 (2014).
[4] A. Richter, M. Koch, T. Matsuyama, Ch. Heyn, and U. Merkt, Appl. Phys. Lett. **77**, 3227 (2000).
[5] Ch. Heyn, S. Mendach, S. Löhr, S. Beyer, S. Schnüll, and W. Hansen, J. Crist. Growth **251**, 832 (2003).
[6] C.H. Möller, Ch. Heyn, and D. Grundler, Appl. Phys. Lett. **83**, 2181 (2003).
[7] M. Hirmer, D. Schuh, and W. Wegscheider, Appl. Phys. Lett. **98**, 082103 (2011).
[8] K. Tsumura, S. Nomura, T. Akazaki, and J. Nitta, Phys. E **34**, 315 (2006).
[9] Ya.V. Terent'ev, S.N. Danilov, H. Plank, J. Loher, D. Schuh, D. Bougeard, D. Weiss, M.V. Durnev, S.A. Tarasenko, I.V. Rozhansky, S.V. Ivanov, D.R. Yakovlev and S.D. Ganichev, J. Appl. Phys. **34**, 113906 (2015).
[10] C.-M. Hu, C. Zehnder, Ch. Heyn, and D. Heitmann, Phys. Rev. B **67**, 201302(R) (2003).
[11] J. Nitta, Y. Lin, T. Akazaki, and T. Koga, Appl. Phys. Lett. **83**, 4565 (2003).
[12] U. Wurstbauer, M. Soda, R. Jakiela, D. Schuh, D. Weiss, J. Zweck, W. Wegscheider, J. of Cryst. Growth **311**, 2160 (2009).

[13] U. Wurstbauer, S. Sliwa, D. Weiss, T. Dietle, and W. Wegscheider, Nature Physics **6**, 955 (2010).
[14] S.D. Ganichev, S.A. Tarasenko, V.V. Bel'kov, P. Olbrich, W. Eder, D.R. Yakovlev, V. Kolkovsky, W. Zaleszczyk, G. Karczewski, T. Wojtowicz, and D. Weiss, Phys. Rev. Lett. **102**, 156602 (2009).
[15] P. Olbrich, C. Zoth, P. Lutz, C. Drexler, V.V. Bel'kov, Ya. V. Terent'ev, S.A. Tarasenko, A.N. Semenov, S.V. Ivanov, D.R. Yakovlev, T. Wojtowicz, U. Wurstbauer, D. Schuh, and S.D. Ganichev, Phys. Rev. B **85**, 085310 (2012).
[16] F. Capotondi, G. Biasiol, D. Ercolani, V. Grillo, E. Carlino, F. Romanato, and L. Sorba, Thin Solid Films **484**, 400 (2005).
[17] V.V. Bel'kov and S.D. Ganichev, Semicond. Sci. and Tech. **23**, 114003 (2008).
[18] Chongyun Jiang, V.A. Shalygin, V.Yu. Panevin et al, Phys. Rev. B **84**, 125429 (2011).
[19] P.D. Wang, N.N. Ledentsov, C.M. Sotomayor Torres, I.N. Yassievich, A. Pakhomov, A.Yu. Egovov, P.S. Kop'ev, and V.M. Ustinov, Phys. Rev. B **50**, 1604 (1994).
[20] Mitsuru Sugawara, Yoshiaki Nakata, Kohki Mukai, and Hajime Shoji, Phys. Rev. B **55**, 13155 (1997).
[21] S. N. Walck and T. L. Reinecke, Phys. Rev. B **57**, 9088 (1998).
[22] N.J. Traynor, R.J. Warburton, M.J. Snelling, R.T. Harley, Phys. Rev. B **55**, 15701 (1997).
[23] M. V. Durnev, M. M. Glazov, and E. L. Ivchenko, Phys. Rev. B **89**, 075430 (2014).
[24] M.V. Durnev, Phys. Solid State **56**, 1416 (2014).
[25] I. Vurgaftman, J.R. Meyer, and L.R. Ram-Mohan, Jour. of Appl. Phys. **89**, 5815 (2001).
[26] C.G. Van de Walle, Phys. Rev. B **39**, 1871 (1989).
[27] J.-M. Jancu, R. Scholz, E. A. de Andrada e Silva, and G. C. L. Rocca, Phys. Rev. B **72**, 193201 (2005).
[28] S.N. Danilov, Ya.V. Terent'ev, J. Loher, D. Bougeard, D. Weiss, M.V. Durnev, S.V. Ivanov and S.D. Ganichev, 23rd Int. Symp. Nanostructures: Physics and Technology, Saint Petersburg, Russia, June 22-26, 2015. (NC.02o)
[29] A. V. Malyshev, I. A. Merkulov, and A. V. Rodina, Phys. Stat. Solidi B **210**, 865 (1998).
[30] B. L. Gelmont and M. I. Dyakonov, Fiz. Tekh. Poluprov. **7**, 2013 (1973) [Soviet Phys. Semicond. **7**, 1345 (1974)].
[31] E. L. Ivchenko, *Optical spectroscopy of semiconductor nanostructures* (Alpha Science Internat., Harrow, UK, 2005).
[32] X. Marie, T. Amand, P. Le Jeune, M. Paillard, P. Renucci, L. E. Golub, V. D. Dymnikov, and E. L. Ivchenko, Phys. Rev. B **60**, 5811 (1999).